

UC Irvine

UC Irvine Previously Published Works

Title

Results on neutrino mass and mixing from Super Kamiokande

Permalink

<https://escholarship.org/uc/item/0dj2r5nd>

Journal

Acta Physica Polonica B, 33(1)

ISSN

0587-4254

Authors

Kielczewska, Danuta
Super Kamiokande Collaboration, .
K2K Collaboration, .

Publication Date

2002

Copyright Information

This work is made available under the terms of a Creative Commons Attribution License, available at <https://creativecommons.org/licenses/by/4.0/>

Peer reviewed

RESULTS ON NEUTRINO MASS AND MIXING FROM SUPERKAMIOKANDE*

DANUTA KIELCZEWSKA

for the SuperKamiokande and K2K Collaborations

Institute for Experimental Physics, Warsaw University
and Institute for Nuclear Studies
Hoża 69, 00-681 Warsaw, Poland
e-mail: danka@fuw.edu.pl
and Physics Department, University of California
Irvine, CA 92697, USA

(Received December 28, 2001)

After the discovery of neutrino oscillations by SuperKamiokande three years ago the measurements of their masses and flavor mixing are under way using various neutrino sources and energies. High precision data on atmospheric neutrinos show that the dominant mixings occur between active species. They allow for statistically significant three-flavor analysis, which confirm the almost maximal mixing $\nu_\mu \leftrightarrow \nu_\tau$. Results of searches for tau neutrinos are consistent with this scenario. The K2K experiment, which uses the KEK accelerator as the neutrino source and the SuperKamiokande for their detection, is sensitive to the oscillations observed in the atmospheric neutrinos. The results obtained after one year of the run time provide a check of the oscillation parameters with the well determined beam properties using a set of near detectors and beam monitors. The solution of the solar neutrino puzzle in terms of ν_e oscillations has been recently much enhanced by exciting new results from the SNO Collaboration. Their comparison with SuperKamiokande results again excludes a sterile neutrino mixing as dominant suggesting instead a large ν_e mixing with other active neutrinos. This interpretation has been favored by recent SuperKamiokande spectral and angular measurements.

PACS numbers: 14.60.Pq, 14.60.Lm, 95.30.Cq, 95.55.Vj

* Presented at the XXVII Mazurian Lakes School of Physics, Krzyże, Poland, September 2–9, 2001.

1. Introduction

One of the most fundamental tasks of particle physics is a determination of neutrino masses. The only currently used technique allowing to probe mass scales smaller than 1 eV is neutrino oscillation, discovered three years ago by the SuperKamiokande Collaboration [1–3]. The fascinating history of searches for neutrino oscillations and many experimental details can be found in review articles in Refs. [4, 5].

The oscillation probability depends on the ratio of the distance traveled by neutrinos to their energy and on the difference of masses of participating neutrino states. The SuperKamiokande (SK) experiment is sensitive to wide range of mass differences because it can study both the neutrinos produced in the Earth atmosphere and much less energetic neutrinos resulting from thermonuclear reactions in the solar core. It uses a large water Cherenkov detector located underground in the Kamioka mine in Japan. It contains 50 kton of ultra-pure water and is equipped with 11134 50 cm photomultiplier tubes. It has operated with over 90% live time since April 1996 until July 2001. We report here the data analysis for almost 80 kiloton-year exposure.

In Sec. 2 we will show formulae relevant for mixing of three neutrino flavors and approximations which allow for a decoupling of the oscillation analysis of atmospheric and solar data.

The results on atmospheric neutrinos are described in Sec. 3. The data samples are large enough to allow for 3-flavor analysis, a better discrimination between $\nu_\mu \leftrightarrow \nu_\tau$ and $\nu_\mu \leftrightarrow \nu_{\text{sterile}}$ hypotheses and first results on ν_τ appearance searches.

The SK detector registers also neutrinos produced at the KEK accelerator 250 km away. The experiment is able to probe the $\nu_\mu \leftrightarrow \nu_x$ oscillation parameters derived from atmospheric neutrinos. The data obtained until March 2001 are described in Sec. 4.

The solar neutrino deficit puzzle is much closer to its final solution with the new data from Sudbury Neutrino Observatory (SNO) and their comparison with SK measurements. In Sec. 5 we summarize the data as well as an oscillation analysis of all available solar neutrino results.

Earlier results on atmospheric and solar results, as well as the very first data from K2K experiment were described in Ref. [6], where the reader can find more details and explanations about the experiments as well as procedures used in the data analysis.

2. Neutrino oscillations

Mixing of 3 active neutrinos is described by a 3×3 matrix, analogous to the Cabibbo–Kobayashi–Maskawa quark matrix. It transforms 3 states with definite masses to 3 states participating in weak interactions. Conventionally the parametrization advocated by Particle Data Group [7] is used.

$$V = \begin{pmatrix} c_{12}c_{13} & s_{12}c_{13} & s_{13}e^{-i\delta} \\ -s_{12}c_{23} - c_{12}s_{13}s_{23}e^{-i\delta} & c_{12}c_{23} - s_{12}s_{13}s_{23}e^{i\delta} & c_{13}s_{23} \\ s_{12}s_{23} - c_{12}s_{13}c_{23}e^{i\delta} & -c_{12}s_{23} - s_{12}s_{13}c_{23}e^{i\delta} & c_{13}c_{23} \end{pmatrix},$$

where $s_{ik} = \sin(\theta_{ik})$, $c_{ik} = \cos(\theta_{ik})$

Assuming CP conservation: ($\delta = 0$) the transformation from the mass eigenstates ν_1, ν_2, ν_3 to the flavor states ν_e, ν_μ, ν_τ is expressed by 3 rotation matrices:

$$\begin{pmatrix} \nu_e \\ \nu_\mu \\ \nu_\tau \end{pmatrix} = \begin{pmatrix} 1 & 0 & 0 \\ 0 & c_{23} & s_{23} \\ 0 & -s_{23} & c_{23} \end{pmatrix} \begin{pmatrix} c_{13} & 0 & s_{13} \\ 0 & 1 & 0 \\ -s_{13} & 0 & c_{13} \end{pmatrix} \begin{pmatrix} c_{12} & s_{12} & 0 \\ -s_{12} & c_{12} & 0 \\ 0 & 0 & 1 \end{pmatrix} \begin{pmatrix} \nu_1 \\ \nu_2 \\ \nu_3 \end{pmatrix}.$$

The probability of oscillations is then given by:

$$P(\nu_\alpha \rightarrow \nu_\beta) = -2 \sum_{i=1}^3 \sum_{j=1, j \neq i}^3 V_{\alpha i} V_{\beta i} V_{\alpha j} V_{\beta j} \sin^2 \left(\frac{1.27 \delta m_{ij}^2 L}{E_\nu} \right),$$

where $\delta m_{ij}^2 = m_i^2 - m_j^2$, L is the neutrino pathlength and E_ν its energy.

With three different masses m_i one has two independent differences, *e.g.* $\delta m_{12} \equiv \delta m$ and $\delta m_{23} \equiv \Delta m$. In a likely scenario that $\Delta m \gg \delta m$, one can approximate $\delta m_{13} \approx \delta m_{23}$.

Now suppose that we have two experimental conditions, in which the measured L/E values are significantly different. Then for relatively small values of L/E_ν (*e.g.* in case of atmospheric neutrinos) one can make the following approximation:

$$\sin^2 \left(\frac{1.27 \delta m^2 L}{E_\nu} \right) \approx 0.$$

With this one gets the following transformation probabilities:

$$P(\nu_\mu \rightarrow \nu_\tau) = \cos^4(\theta_{13}) \sin^2(2\theta_{23}) \sin^2 \left(\frac{1.27 \Delta m^2 L}{E_\nu} \right), \quad (1)$$

$$P(\nu_\mu \rightarrow \nu_e) = \sin^2(2\theta_{13}) \sin^2(\theta_{23}) \sin^2 \left(\frac{1.27 \Delta m^2 L}{E_\nu} \right), \quad (2)$$

$$P(\nu_e \rightarrow \nu_\tau) = \sin^2(2\theta_{13}) \cos^2(\theta_{23}) \sin^2 \left(\frac{1.27 \Delta m^2 L}{E_\nu} \right). \quad (3)$$

On the other hand in the case of solar neutrino experiments the approximation of large L/E_ν is useful:

$$\left\langle \sin^2 \left(\frac{1.27 \Delta m^2 L}{E_\nu} \right) \right\rangle \approx 0.5.$$

Then:

$$P(\nu_e \rightarrow \nu_e) = 1 - \cos^4(\theta_{13}) \sin^2(2\theta_{12}) \sin^2 \left(\frac{1.27 \delta m^2 L}{E_\nu} \right) - 0.5 \sin^2(2\theta_{13}). \quad (4)$$

Thus for well separated mass squared one gets “a decoupling” of the oscillation analysis.

In case of a small angle θ_{13} the above formulae lead to the well known expression for oscillation probability in 2-flavor case:

$$P_{i \rightarrow f} = \sin^2 2\theta \sin \left(\frac{1.27 \Delta m^2 (\text{eV}^2) L (\text{km})}{E_\nu (\text{GeV})} \right). \quad (5)$$

3. Atmospheric neutrinos

Atmospheric neutrinos¹ are produced by cosmic rays with in the Earth atmosphere. As a result of a power-law momentum spectrum of primary cosmic rays the neutrinos have mostly energies of a few GeV. In a large underground detector they give rise to the interactions occurring inside the fiducial volume of the detector, called *contained* events. The events are called Fully Contained (FC) if charged products do not leave the inner detector volume, otherwise they are classified as Partially Contained (PC).

The FC events of the SK sample are additionally subdivided into “sub-GeV” (with visible energy <1.33 GeV) and “multi-GeV” (>1.33 GeV) events.

One can significantly increase statistics of high energy neutrinos taking into account interactions occurring in the rock outside of the detector with muons entering the detector fiducial volume. Due to the large background of the downward-going cosmic ray muons the neutrino-induced events can be selected only if they produce *upward-going muons*. The upward-going muons can either traverse the entire detector (“through-going”) or stop inside of it.

The data are compared with detailed MC simulations of neutrino interactions and detector response. The simulations are done for fluxes calculated by Honda *et al.* [8], Bartol group [9] and Battistoni *et al.* [10].

¹ Throughout the section about atmospheric neutrinos we tacitly assume a sum of neutrinos and antineutrinos when we write about *neutrinos*.

3.1. Contained events

The contained event rates measured in a 79 kiloton-year exposure (or 1289 days of detector lifetime) are compared with those expected from Monte Carlo simulations in Table I. One can clearly see the known for more than a decade deficit of muon neutrinos, which are detected mostly as μ -like events.

TABLE I

Sample of contained events (1289 days).

	Sub-GeV		Multi-GeV	
	Data	MC	Data	MC
Single track:				
e -like	2864	2668	626	613
μ -like	2788	4073	558	838
PC μ -like			754	1065
Multi track	2159	2585	1318	1648
Total	7811	9326	3256	4164

The measured flavor ratio is conventionally compared to expectation as the “ratio of ratios”, R , defined as

$$R = \frac{(N_\mu/N_e)_{\text{DATA}}}{(N_\mu/N_e)_{\text{MC}}}, \quad (6)$$

where N_μ and N_e are numbers of μ -like and e -like single track events for data and MC. For no oscillations, R is expected to be 1, while the measured double ratio is $0.638 \pm 0.017(\text{stat.}) \pm 0.050(\text{syst.})$ for sub-GeV and $0.675 \pm 0.034(\text{stat.}) \pm 0.080(\text{syst.})$ for multi-GeV samples.

At energies relevant for atmospheric neutrinos there is no significant flux attenuation in Earth and so an approximate up-down symmetry is expected. We then compare the experimental and theoretical distributions of zenith angle for different event categories. In Fig. 1 $\cos \theta = -1$ corresponds to upward-going neutrinos. A deficit of muon neutrinos passing through the Earth clearly seen, while the observed angular distribution of e -like events agrees in shape with simulations.

3.2. Upward-going muons

The upward-going muon sample makes it possible to probe higher neutrino energies. With an interaction point outside of the detector the event energy cannot be measured. However, a relative rate of stopping to through-going events compared to MC expectations provides an independent information about energy dependence of the oscillations. The analysis of earlier

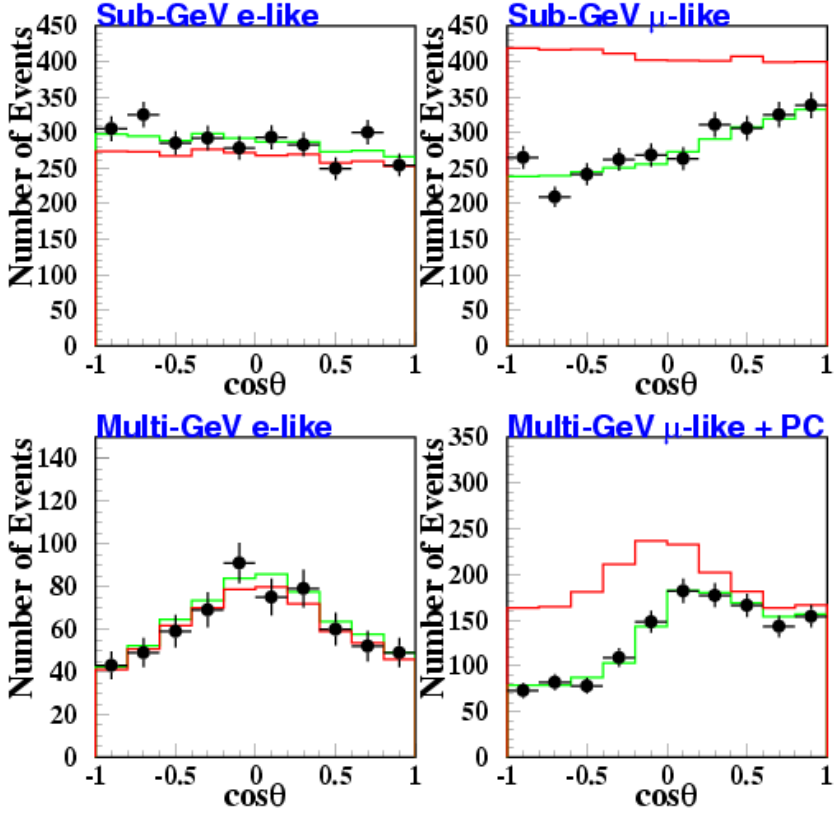


Fig. 1. Angular distributions for sub-GeV (top) and multi-GeV (bottom) 1289 day samples; left figures are for e -like and right for μ -like events. Solid lines show the MC no-oscillation prediction, while broken lines show the $\nu_\mu \leftrightarrow \nu_\tau$ oscillation prediction for the best-fit parameters.

data has been published in Ref. [11,12]. The most recent results are given in Table II. From the comparison of the measured and expected fluxes one again sees a deficit of muons. The measured ratio of stopping to through-going muons, $\mathcal{R} = 0.242 \pm 0.017^{+0.013}_{-0.011}$ has been obtained, significantly smaller than the expected $\mathcal{R} = 0.37 \pm 0.05$ for both Bartol and Honda flux calculations.

TABLE II

Sample of upward-going muons.

Sample	Lifetime (days)	Number of events	Flux ($\times 10^{-13} \text{cm}^{-2} \text{s}^{-1} \text{sr}^{-1}$)		
			Measured	Honda	Bartol
Through-going	1268	1406	1.70 ± 0.05	1.84 ± 0.41	1.97 ± 0.44
Stopped	1247	322	0.41 ± 0.03	0.68 ± 0.15	0.73 ± 0.16

In the high energy events the muon direction is very well correlated with that of a parent neutrino. Fig. 2 shows the flux of through-going muons and the relative fraction of stopping upward muons as functions of zenith angle. They are compared with corresponding MC predictions using the Bartol neutrino fluxes.

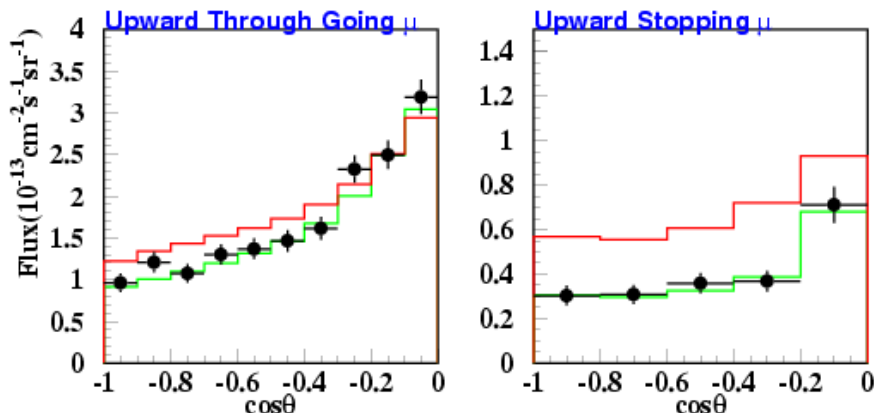


Fig. 2. Zenith angle distribution of upward-going muons. Left: fluxes of through-going muons. Right: the ratio of stopped to through-going muons. The data points are compared with the no-oscillation flux predictions (solid lines), and the best fit $\nu_\mu \leftrightarrow \nu_\tau$ oscillations (the dashed lines).

3.3. Oscillation analysis — two flavor approximation

Fig. 1 shows that the most natural explanation of the observed deficit of upward going muon neutrinos is offered by the $\nu_\mu \leftrightarrow \nu_\tau$ oscillations. At neutrino energies below 10 GeV the Charged Current (CC) cross-section for ν_τ is significantly smaller than that for ν_μ interactions due to the τ lepton mass. On the other hand the shape of the angular distribution of e -like events agrees well with simulations, so transitions $\nu_\mu \leftrightarrow \nu_e$ cannot be significant for the Δm range which can be probed by atmospheric neutrinos. It then follows from Eqs. (2) and (3) that the angle θ_{13} is small compared to θ_{23} . Therefore, we first fit data with the formula (5) with only 2 oscillation parameters: Δm^2 and $\sin^2 2\theta = 1.0$.

A minimal χ^2 analysis is applied to all the data on energy and directions of the contained single ring events and upward-going muons. Additional terms in the χ^2 take into account systematic uncertainties. The flux normalization is treated as a free parameter. The details of the procedure are described in [1, 14].

Assuming $\nu_\mu \leftrightarrow \nu_\tau$ oscillations the best fit is obtained for $\sin^2 2\theta = 1.0$ and $\Delta m^2 = 2.5 \times 10^{-3} \text{ eV}^2$, with $\chi^2/\text{d.o.f.} = 142/152$, while for no-oscillation hypothesis it is 344/154. The histograms for the best fit parameters are superimposed in Fig. 1 and 2. The acceptable oscillation parameters at different confidence levels are delineated by the contours in Fig. 3.

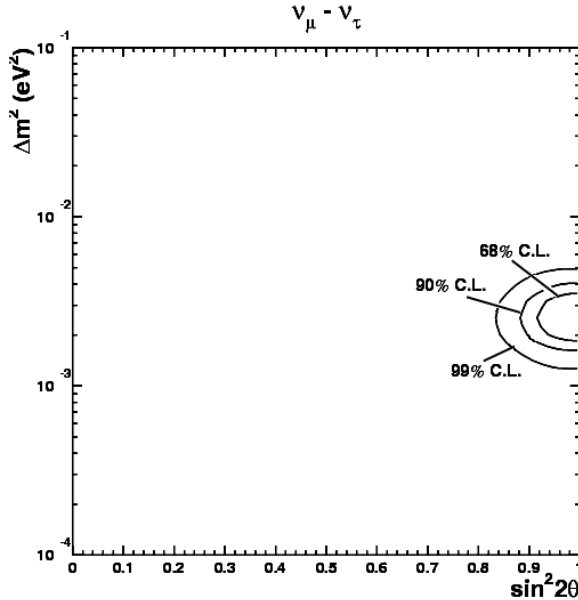


Fig. 3. Allowed regions for parameters of $\nu_\mu \leftrightarrow \nu_\tau$ oscillations using combined information from the contained events and upward-going muons in the SuperKamiokande detector.

Note that using 3-dimensional calculations of neutrino fluxes [10] the best fit is obtained for practically the same parameters: $\sin^2 2\theta = 1.0$ and $\Delta m^2 = 2.4 \times 10^{-3} \text{ eV}^2$.

3.4. Oscillation analysis — three flavor procedure

Large accumulated statistics of data allow for meaningful fit of 3 parameters: Δm^2 , $\sin^2 \theta_{23}$ and $\sin^2 \theta_{13}$ using formulae (2) and (3).

The analysis is performed for contained single track μ -like and e -like events. The best fit results are consistent with 2 flavor analysis, *i.e.* maximum $\nu_\mu \leftrightarrow \nu_\tau$ mixing, $\Delta m^2 = 0.003 \text{ eV}^2$ and $\sin(\theta_{13}) = 0$. Note that here $\sin^2(\theta_{23})$ is displayed instead of $\sin^2(2\theta_{23})$. Regions of the parameters allowed at different c.l. are shown in Fig. 4. The $\nu_\mu \leftrightarrow \nu_e$ transitions at Δm^2 of the order of 10^{-3} eV^2 can be studied with the best sensitivity by search-

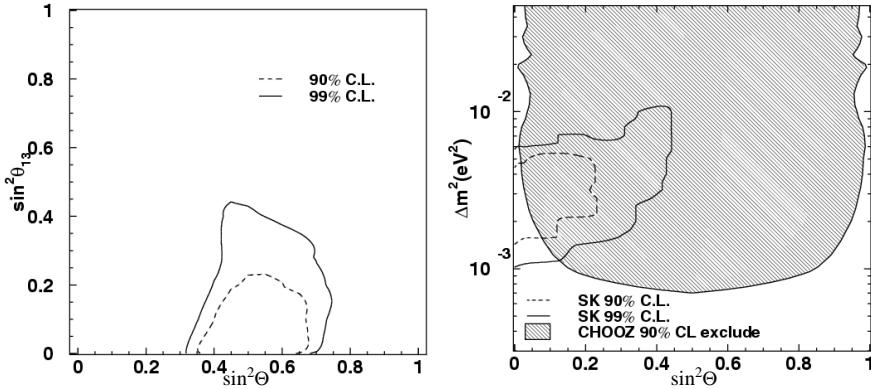


Fig. 4. Allowed regions assuming transitions between 3 active neutrinos. Left: $\sin^2(\theta_{13})$ versus $\sin^2(\theta_{23})$. Right: Δm^2 versus $\sin^2(\theta_{13})$. The shaded area is excluded by Chooz experiment.

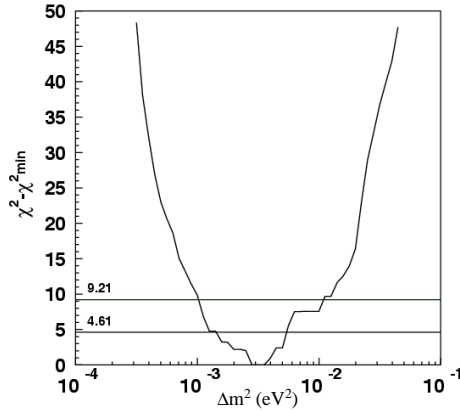


Fig. 5. χ^2 versus Δm^2 in the 3-generation analysis. The lines indicate limits at 90% and 99% c.l.

ing for a disappearance of $\bar{\nu}_e$ in reactor experiments. The best results have been obtained by the Chooz Collaboration [13] and their exclusion limits are superimposed.

The sensitivity of the experiment to the Δm^2 with current statistics is shown in Fig. 5.

3.5. Oscillations into ν_{sterile}

It is interesting to consider also transitions into “sterile” neutrinos which by definition do not interact. The $\nu_\mu \leftrightarrow \nu_{\text{sterile}}$ oscillations can also reproduce the data presented in Fig. 1 [14].

In order to discriminate between pure $\nu_\mu \leftrightarrow \nu_\tau$ and $\nu_\mu \leftrightarrow \nu_{\text{sterile}}$ transitions the following two approaches are possible.

First one can try to select a sample of Neutral Current (NC) interactions. The $\nu_\mu \leftrightarrow \nu_\tau$ transition would not cause any change in this sample because the NC cross sections are the same for ν_τ and for ν_μ . On the other hand one would expect a reduced rate of NC events in case of $\nu_\mu \leftrightarrow \nu_{\text{sterile}}$ oscillations. On the basis of a simulated sample a set of cuts has been determined which enhances a contribution of NC interactions among multi-ring events of the

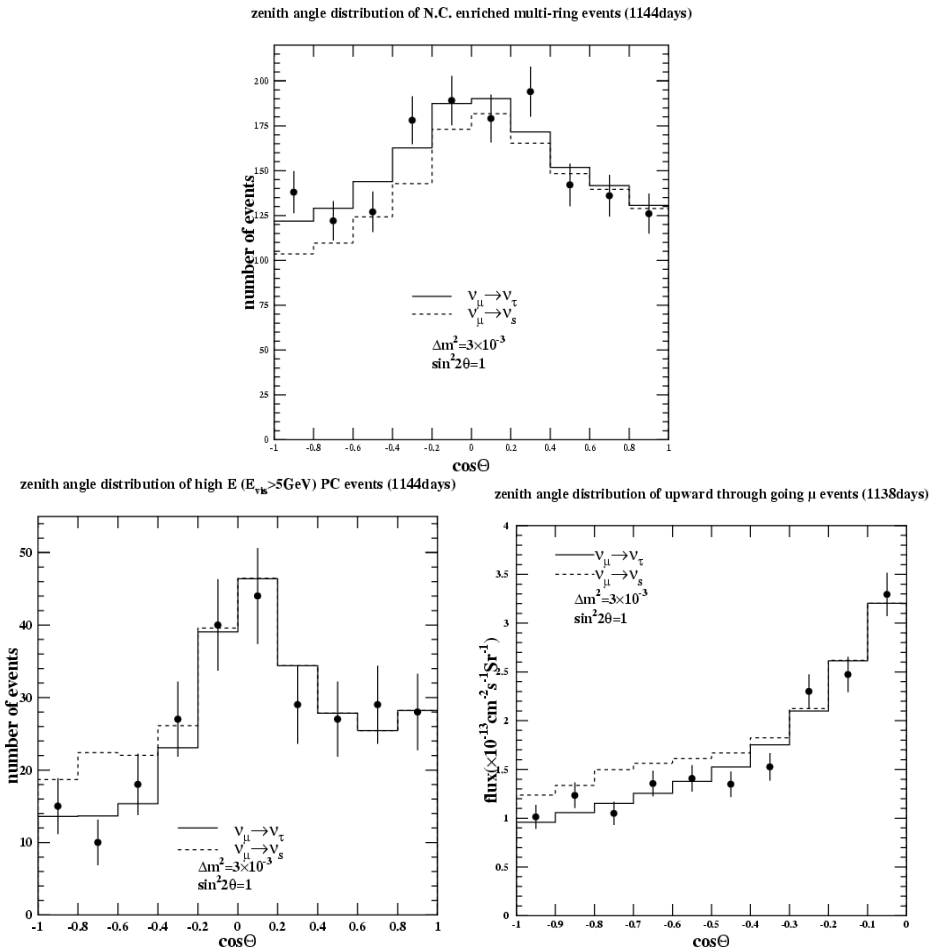


Fig. 6. Zenith angle distributions. Top: multi-ring sample enriched in neutral current interactions; Bottom: PC sample (left) and upward-going muons (right). The histograms correspond to $\nu_\mu \leftrightarrow \nu_\tau$ (solid) and $\nu_\mu \leftrightarrow \nu_{\text{sterile}}$ (dashed) oscillations with the mixing parameters indicated in the figure.

SK data. The zenith angle distribution of the data is compared in Fig. 6 (top) with expectations for both $\nu_\mu \leftrightarrow \nu_\tau$ and $\nu_\mu \leftrightarrow \nu_{\text{sterile}}$. It is seen that the $\nu_\mu \leftrightarrow \nu_\tau$ oscillations fit better the data.

Another approach is to select a sample of charge current interactions in the detector and exploit the matter effects in Earth [16]. During the neutrino passage through Earth the ν_μ and ν_τ undergoes a “refraction” because of the NC interactions with matter. The effect is the same for both flavors. On the other hand the difference in interactions for ν_μ and ν_{sterile} leads to a potential term in the difference of energies of propagating neutrinos and consequently to different velocities. The effect appears to be stronger for higher neutrino energies and, therefore, samples of PC events and upward-going muons are more suitable for this study. The zenith angle distributions for both samples are also displayed in Fig. 6. Again it is seen that the ν_{sterile} hypothesis is less likely.

As a result of the statistical analysis of all the three independent data samples pure $\nu_\mu \leftrightarrow \nu_{\text{sterile}}$ oscillations are disfavored at 99% c.l. The details of the analysis are described in Ref. [15, 17] but the results presented here have been obtained with larger samples (1144 days for multi-ring and PC samples and 1138 days for upward-muons).

3.6. Search for ν_τ appearance

The spectrum of atmospheric neutrinos is too soft for a significant number of CC ν_τ interactions. However for the maximal mixing and $\Delta m^2 = 0.003 \text{ eV}^2$ one expects 74 ν_τ events from the $\nu_\mu \leftrightarrow \nu_\tau$ oscillations for 79 kton-year exposure. The basic distinction of ν_τ events from the background of muon and electron atmospheric neutrinos comes from higher event energies and larger number of tracks, because tau lepton decays add to the total number of pions in an event. Three different techniques were undertaken in order to select samples enriched in tau events. They were optimized using MC and data samples for downgoing neutrinos in which no signal is expected. Thus determined procedures were then applied to the whole samples. Here we present some preliminary results [18].

Fig. 7 shows the zenith angle distributions for a tau enriched sample selected by one of the analysis. The data are compared with 2 histograms of simulated samples. The solid one is for the background of atmospheric neutrinos (BG) normalized by the exposure. Dotted histogram is a sum of BG and ν_τ sample, but the normalization of both samples is obtained by a 2-parameter fit to the data sample.

The results are shown in Table III. It is seen that the results of different analysis are consistent with ν_τ appearance at about 2 sigma level. However it has to be noted that all 3 analysis are based on the same MC simulations.

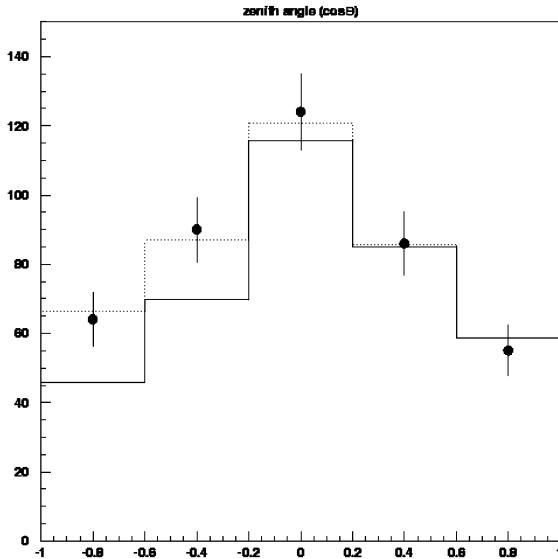


Fig. 7. Zenith angle distribution for a sample enriched in ν_τ events. Dots denote data and histograms simulated samples (see the text).

TABLE III

Summary of the ν_τ search

Analysis	1	2	3
Number of $CC\nu_\tau$	$43 \pm 17^{+8}_{-11}$	$44 \pm 20^{+8}_{-12}$	25.5^{+14}_{-13}
Efficiency	0.42	0.45	0.32
Number of CC ν_τ (efficiency corrected)	$103 \pm 41^{+18}_{-26}$	$98 \pm 44^{+18}_{-27}$	79^{+44}_{-40}

4. Accelerator neutrinos — K2K experiment

The K2K experiment is the first long-baseline neutrino-oscillation experiment using laboratory neutrinos. Almost a pure ν_μ beam from π^+ decays is generated in the KEK 12 GeV/c Proton Synchrotron, and neutrino events are detected in the SK detector 250 km away.

The experiment sensitivity depends on a precise determination of the original neutrino flux and on the measurement of event rates as well as an energy spectrum modulation in SK. To ensure good understanding of the beam at production a set of three detectors situated at a distance of 80 m from the decay tunnel at KEK is used. It consists of a 1 kton water

Cherenkov detector and a fine-grained detector, which in turn consists of the scintillating fiber detector [19], scintillation counters, a lead-glass counter and a muon range detector [20].

The results on the event rates with 100 days of data taken from June 1999 to June 2000, corresponding to 2.29×10^{19} protons on target are described in Ref. [21]. Here we report the results based on the data collected until the end of March 2001, using the beam of 3.85×10^{19} protons on target [23].

4.1. Event rates

The sample of K2K neutrino events in SuperKamiokande is collected applying the same procedure as that for atmospheric neutrinos and requiring a time correlation with the beam. The beam pulses occur every 2.2 sec with a duration of $1.1 \mu\text{sec}$. The selection of the correlated events is done off-line and is based on the time difference between the neutrino beam spill and each SK event using the Global Positioning System (GPS) [22].

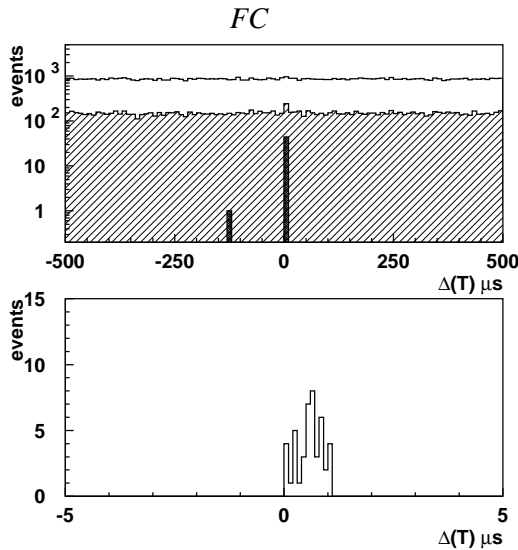


Fig. 8. Time distribution of SuperKamiokande events (FC) with respect to the nearest spill of the beam. The bottom plot shows the distribution of the events within the peak around zero with binning corresponding to the GPS resolution.

The time difference with respect to the nearest spill is shown in Fig. 8 for fully contained events in 22.5 kton fiducial volume. In the top plot 1 msec window covering the neutrino beam period one event out of time with the K2K beam is observed. This is consistent with the expected background from atmospheric neutrinos. The bottom plot in the figure shows an expan-

sion of the central bins of the upper plot. Taking into account an expected accuracy of $< 0.2\mu\text{sec}$ of the absolute time determination, the distribution is in excellent agreement with the beam pulse width.

The peak consists of 44 fully contained interactions in Fiducial Volume (FV) of the inner detector. The details of the sample are shown in Table IV together with the numbers of events expected in each category for non oscillating neutrinos and oscillations with maximum mixing and various Δm^2 .

TABLE IV

Number of observed and expected events in Super Kamiokande.

	Events observed	Events expected $\Delta m^2 (\times 10^{-3} \text{ eV}^2)$			
		No oscillations	3	5	7
FC 22.5 kt	44	$63.9^{+6.1}_{-6.6}$	41.5 ± 4.7	27.4 ± 3.1	23.1 ± 2.6
Single tracks	26	38.4 ± 5.5	22.3 ± 3.4	14.1 ± 2.2	13.1 ± 2.0
μ -like	24	34.9 ± 5.5	19.3 ± 3.2	11.6 ± 1.9	10.7 ± 1.8
e -like	2	3.5 ± 1.4	2.9 ± 1.2	2.5 ± 1.0	2.4 ± 1.0
Multi tracks	18	25.5 ± 4.3	19.3 ± 3.4	13.3 ± 2.3	10.0 ± 1.8

To predict the event rate at the far site we use a normalization measurement of the rate at the near site and an extrapolation of the information about the beam from near to far site. For the rate normalization the data from the 1kton detector are taken so that any detector or analysis systematics are reduced. The extrapolation is based on the beam simulation, which is validated by measurements of pion kinematics in the decay channel.

The results shown in the Table are not yet conclusive, but the number of observed events is by 2σ smaller than expected without oscillations.

4.2. Energy spectrum

As the sample of neutrino interactions in SK associated with the KEK beam is getting larger, the energy distribution can be compared with the neutrino spectrum at production.

The distribution of parent neutrino energy is shown in Fig. 9 for the sample of 24 single track muons observed in SK. It is derived from the muon momenta and their angle with respect to the known neutrino direction assuming that most of them are produced in quasi-elastic interactions, $\nu_\mu N \rightarrow \mu N'$. The histogram shows the prediction obtained by the beam simulation in case of no oscillations. An observed distortion at low energies is consistent with the Δm^2 values obtained from atmospheric neutrinos.

More qualitative conclusions will be made after the studies of systematical errors are completed. Large samples of interactions in the near detectors are currently under study for this purpose.

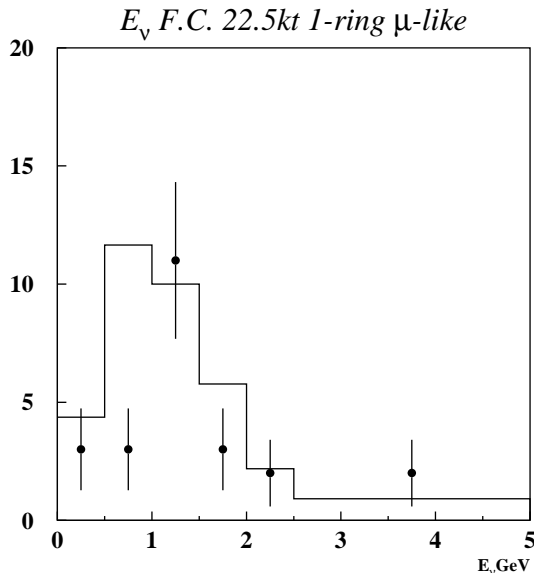


Fig. 9. Spectrum of parent neutrinos for single track muons measured in Super Kamiokande detector. The solid histogram shows the MC spectrum if there were no oscillations.

In conclusion the hypothesis of no oscillations is disfavored at 2σ level based on the observed event rates. Spectral modulation confirms this statement but needs better understanding of systematical errors.

It is hoped that a final integrated beam intensity of 10^{20} protons on target, which was originally planned, will be achieved in future runs providing sufficient statistics for the spectral analysis.

5. Solar neutrinos

Significant deficit of electron neutrinos arriving from the Sun has been now reported by many different experiments [24–30]. No Standard Solar Model (SSM) [31, 32] modifications are able to explain the observed event rates. Moreover with all the available data, especially with the most recent results from SNO, it can now be concluded in a model independent way, that the over 40 years old puzzle of solar ν deficit can be explained by neutrino transformations after their production in the solar core.

5.1. SuperKamiokande data

The data accumulated during 1258 days (77.5 kton-years) were recently published in Ref. [29] so here we give a brief summary of the results.

Solar neutrinos are observed in SK via elastic neutrino–electron scattering in water:

$$\nu_e + e^- \longrightarrow \nu_e + e^- . \quad (7)$$

Due to kinematics of the reaction the electron follows the neutrino direction. Therefore the angle between reconstructed electron direction and the current direction away from the Sun can be used to separate solar neutrino interactions from background events.

As a result $18464 \pm 204(\text{stat.})_{-554}^{+646}(\text{syst.})$ signal events above 5 MeV recoil electron energy have been selected. This is only $45.1 \pm 0.5(\text{stat.})_{-1.4}^{+1.6}(\text{syst.})\%$ of the prediction based on SSM of Ref. [31]. Assuming the ${}^8\text{B}$ spectrum shape of electron neutrinos the integrated flux over all energies is $(2.32 \pm 0.03(\text{stat.}) \pm 0.08(\text{syst.})) \times 10^6 / \text{cm}^2 / \text{sec}$.

If resonant interaction in matter (MSW effect [16]) effect in the solar matter is responsible for a $\nu_e \rightarrow \nu_x$ transition, then for a range of oscillation parameters the $\nu_x \rightarrow \nu_e$ process may occur in the Earth, leading to a regeneration of the electron neutrinos and an increase of the signal during nights. The measured day–night asymmetry is:

$$\frac{2(\text{day} - \text{night})}{\text{day} + \text{night}} = -0.033 \pm 0.022(\text{stat.}) \pm 0.013(\text{syst.})$$

i.e. there is no significant effect.

A modulation of the well known spectrum of neutrinos from ${}^8\text{B}$ decay would be a clear signal of neutrino oscillations. However the measured energy distribution is consistent with no spectral distortion.

5.2. SNO data

Elastic scattering off electrons (7) can proceed via both CC and NC interactions and therefore SK events can be caused by a mixture of ν_e , ν_μ and ν_τ neutrinos.

The Cherenkov detector in Sudbury Neutrino Observatory is filled with heavy water and loosely bound neutrons make it possible to measure pure CC interactions: $\nu_e + d \rightarrow e^- + p + p$. The SNO Collaboration published recently initial results of flux measurements [30] and found a significant deficit of solar ν_e . The ν_e flux integrated over energy assuming the ${}^8\text{B}$ neutrino spectrum shape is: $1.75 \pm 0.07(\text{stat.})_{-0.11}^{+0.12}(\text{syst.}) \pm 0.05(\text{theor.}) \times 10^6 \text{ cm}^{-2} \text{ s}^{-1}$ which is more than 3σ smaller than the ${}^8\text{B}$ flux measured by SK. The difference

is interpreted as a model independent indication of a non-electron flavor component in the solar neutrino flux. When it is ascribed to interactions of $\nu_{\mu\tau}$ with ${}^8\text{B}$ spectrum their integrated flux is $3.7 \pm 1.1 \times 10^6 \text{ cm}^{-2}\text{s}^{-1}$. The sum of all active neutrinos turns out to be very close to predictions of standard solar models.

5.3. Oscillation analysis

The discrepancy between SSM and the flux measurements may be explained by oscillation of electron neutrinos $\nu_e \leftrightarrow \nu_x$ into another neutrino type, which interacts in the detector with much smaller cross section. In particular ν_μ and ν_τ of a few MeV can only scatter on electrons via NC and hence their detection rate is much smaller. Another possibility is an oscillation into a sterile neutrino.

If the δm^2 between dominant components of ν_e and ν_x is very small ($< 10^{-9} \text{ eV}^2$) then the flavor conversion occurs in “vacuum” during the ν_e travel from the Sun to Earth. If δm^2 is larger, then the MSW resonant enhancement causes a flavor transformation in the dense solar matter.

As a real-time solar neutrino experiment, SK can measure the direction (or *zenith angle*) to the Sun and consequently a neutrino pathlength through Earth for every event. The large statistics accumulated by SK allow to measure recoil energy distributions in several bins of the zenith angle. These data strongly constrain the oscillation parameters and allow for a flux independent oscillation analysis. The results of the 1258 day sample have been published in Refs. [33].

It is shown that due to lack of a significant spectrum distortions and zenith angle dependence, “vacuum” solutions and small mixing angles are disfavored. Also the $\nu_e \leftrightarrow \nu_{\text{sterile}}$ transitions do not fit well to the data.

The SNO ν_e flux measurements enhance the preference for large mixing angle solutions. In Fig. 10 the results of a global 2-flavor oscillation analysis are shown [34]. The data used for this analysis consist of event rates measured in Homestake chlorine experiment [24], the gallium experiments: Gallex [26], SAGE [25] and GNO [27], fluxes from SNO and SK as well as SK spectra and zenith angle distributions. The figure shows the regions of parameters allowed for transitions between ν_e and a superposition of ν_μ, ν_τ states ($\nu_e \leftrightarrow \nu_{\mu\tau}$) at various confidence levels. It is seen that at 95% c.l. the only accepted solution is the so called LMA with δm^2 between $3 \times 10^{-5} \text{ eV}^2$ and $2 \times 10^{-4} \text{ eV}^2$ and $\tan^2 \theta$ between 0.2 and 0.7.

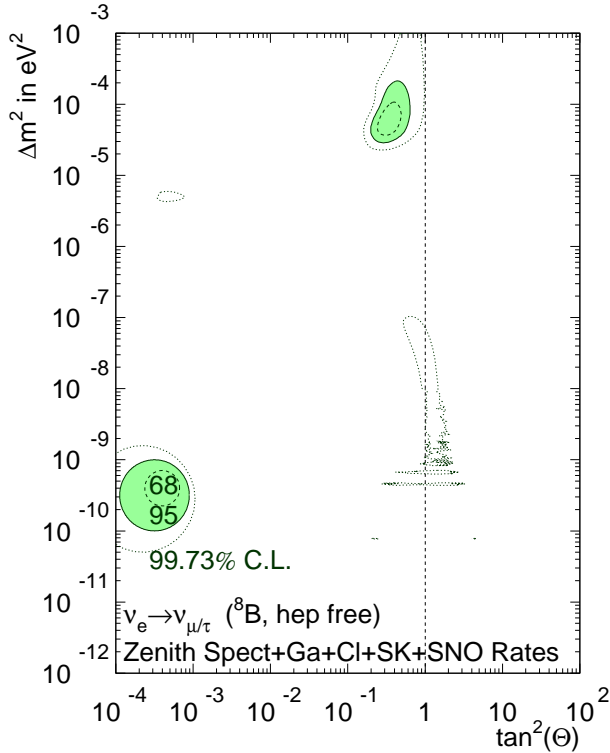


Fig. 10. Regions of accepted oscillation parameters using the event rates of all the solar neutrino experiments as well as spectra and zenith angle distributions from the SuperKamiokande.

6. Summary

Increased samples of atmospheric neutrino interactions confirm the earlier results showing the evidence for muon neutrino oscillations.

The best interpretations of the data is in terms of $\nu_\mu \leftrightarrow \nu_\tau$ flavor transformation with maximal mixing and Δm^2 of 0.003 eV^2 , when mixing between all 3 neutrino flavors is taken into account. However errors allow for the Δm^2 values in a wide range from 0.001 eV^2 to 0.006 eV^2 (at 90% c.l.). Results of searches for ν_τ appearance have provided a positive signal only at 2 sigma level but they are consistent with the $\nu_\mu \leftrightarrow \nu_\tau$ maximal mixing scenario.

Additional support for ν_μ oscillations and the above Δm^2 range of values has been recently provided by the data from the K2K experiment. By itself the signal is only at 2 sigma level, but the initial neutrinos are better defined and their pathlength known very precisely.

The recent solar data obtained by SNO Collaboration cleared significantly the old puzzle of ν_e deficit. When combined with the SK data they strongly suggest that ν_e oscillates to a $\nu_{\mu\tau}$ combination of states. This result is independent of solar models. Moreover the best fits to all the existing data are obtained for large mixing, $\tan^2 \theta > 0.2$, and δm^2 larger than $3 \times 10^{-5} \text{ eV}^2$ with the flavor transformation enhanced by matter effects inside the Sun.

All the experimental data covered in this report show that neutrinos are massive (at least one ν mass is larger than 0.04 eV) and the Standard Model needs to be extended. Moreover maximal mixing interpretations of both atmospheric and solar data provide us with a puzzle of quite different structures of lepton and quark sectors. In order to understand better an origin of the differences one needs further and more precise measurements of full neutrino mass and mixing matrices.

The near future should abound in data from new detectors. The SNO Collaboration has already started to collect the data with salt added to heavy water and thus making it possible to study another NC reaction, $\nu_x + d \rightarrow \nu_x + n + p$. Soon Borexino [35] and KamLAND [36] should be operational. Borexino will hopefully measure the solar ν spectrum down to 250 keV and KamLAND studies of reactor antineutrinos should be sensitive to large mixing at $\delta m^2 > 10^{-5} \text{ eV}^2$.

Several new long-baseline experiments are dedicated to investigate the $\nu_\mu \leftrightarrow \nu_x$ oscillations observed in atmospheric neutrinos, using the accelerator beams. The MINOS experiment [37] will use the Fermilab intense ν_μ beam. At CERN the ν_μ beam will be directed to Gran Sasso, where 2 detectors: ICARUS [38] and OPERA [39] are designed to observe ν_τ appearance.

Moreover first data are soon expected from the Mini-Boone experiment [40], which should confirm or refute the LSND results [41] indicating possible $\nu_\mu \leftrightarrow \nu_e$ oscillations in the $mass^2$ difference above 1 eV^2 , *i.e.* at much higher scale than discussed in this paper.

The SuperKamiokande detector has been seriously damaged recently, causing an unexpected break in the operation of SK and K2K experiments. At the moment it is hoped that the SK will be rebuilt, most likely with a smaller PMT density, which should not be detrimental to studies of atmospheric neutrinos and K2K.

The SuperKamiokande and K2K experiments are supported by the Japanese Ministry of Education, Science, Sports and Culture and the United States Department of Energy. The author gratefully acknowledges the support of the Polish State Committee for Scientific Research (KBN) under grant no 5P0309520. The author is thankful to the organizers for kind invitation and hospitality extended to her at the workshop.

REFERENCES

- [1] Y. Fukuda *et al.*, *Phys. Rev. Lett.* **81**, 1562 (1998).
- [2] Y. Fukuda *et al.*, *Phys. Lett.* **B433**, 9 (1998).
- [3] Y. Fukuda *et al.*, *Phys. Lett.* **B436**, 33 (1998).
- [4] T. Kajita, Y. Totsuka, *Rev. Mod. Phys.* **73**, 85 (2001).
- [5] J.G. Learned, [hep-ex/0007056](#).
- [6] D. Kielczewska [SuperKamiokande and K2K Collaborations], *Acta Phys. Pol.* **B31**, 1181 (2000).
- [7] D.E. Groom *et al.*, *Eur. Phys. J. C* **15**, 1 (2000).
- [8] M. Honda *et al.*, *Phys. Lett.* **B248**, 193 (1990); *Phys. Rev.* **D52**, 4985 (1995); *Prog. Theor. Phys. Suppl.* **123**, 483 (1996).
- [9] G. Barr *et al.*, *Phys. Rev.* **D39**, 3532 (1989); V. Agrawal *et al.* *Phys. Rev.* **D53**, 1314 (1996).
- [10] G. Battistoni *et al.*, *Astropart. Phys.* **12**, 315 (2000).
- [11] Y. Fukuda *et al.*, *Phys. Rev. Lett.* **82**, 2644 (1999).
- [12] Y. Fukuda *et al.*, *Phys. Lett.* **B467**, 185 (1999).
- [13] M. Apollonio *et al.*, *Phys. Lett.* **B420**, 397 (1998); *Phys. Lett.* **B466**, 415 (1999).
- [14] M.D. Messier, PhD thesis, Boston University 1999.
- [15] K. Ishihara, PhD Thesis, University of Tokyo, Dec. 1999.
- [16] S.P. Mikheev, A.Y. Smirnov, *Sov. Journ. Nucl. Phys.* **42**, 913 (1985); *Nuovo Cim.* **9C**, 17 (1986); L. Wolfenstein, *Phys. Rev.* **D17**, 2369 (1978).
- [17] S. Fukuda *et al.*, *Phys. Rev. Lett.* **85**, 3999 (2000).
- [18] for more details see T. Toshito [SuperKamiokande Collaboration], [hep-ex/0105023](#).
- [19] A. Suzuki *et al.*, *Nucl. Instrum. Methods Phys. Res.* **A453**, 165 (2000).
- [20] T. Ishii *et al.*, [hep-ex/0107041](#).
- [21] S.H. Ahn *et al.* [K2K Collaboration], *Phys. Lett.* **B511**, 178 (2001).
- [22] H.G. Berns, R.J. Wilkes. *IEEE Trans. Nucl. Sci.* **47**, 340 (2000).
- [23] for more details see J.E. Hill [K2K Collaboration], [hep-ex/0110034](#).
- [24] B. Cleveland *et al.* [Homestake Collaboration], *Astrophys. J.* **496**, 505 (1998).
- [25] V. Gavrin [SAGE Collaboration], *Nucl. Phys. B (Proc. Suppl.)* **91**, 36 (2001).
- [26] W. Hampel *et al.* [Gallex Collaboration], *Phys. Lett.* **B447**, 127 (1999).
- [27] E. Bellotti [GNO Collaboration], *Nucl. Phys. B (Proc. Suppl.)* **91**, 44 (2001); M. Altmann *et al.*, *Phys. Lett.* **B490**, 16 (2000).
- [28] Y. Fukuda *et al.* [Kamiokande Collaboration], *Phys. Rev. Lett.* **77**, 1683 (1996).
- [29] S. Fukuda *et al.* [SuperKamiokande Collaboration], *Phys. Rev. Lett.* **86**, 5651 (2001).

- [30] Q.R. Ahmad *et al.* [SNO Collaboration], *Phys. Rev. Lett.* **87**, 071301 (2001);
- [31] J.N. Bahcall, M.H. Pinsonneault, S. Basu, *Astrophys. J.* **555**, 990 (2001).
- [32] A.S. Brun, S. Turck-Chieze, P. Morel, *Astroph. J.* **506**, 913 (1998).
- [33] S. Fukuda *et al.*, *Phys. Rev. Lett.* **86**, 5656 (2001).
- [34] for details see: M.B. Smy, [SuperKamiokande Collaboration], hep-ex/0106064; M.B. Smy hep-ex/0108053.
- [35] G. Alimonti *et al.* [Borexino Collaboration], *Astropart. Phys.* **16**, 205 (2002).
- [36] A. Piepke [KamLAND Collaboration], *Nucl. Phys. B (Proc. Suppl.)* **91**, 99 (2001).
- [37] S.G. Wojcicki [MINOS Collaboration], *Nucl. Phys. B (Proc. Suppl.)* **91**, 216 (2001).
- [38] F. Arneodo *et al.* [ICARUS Collaboration], hep-ex/0103008.
- [39] see <http://operaweb.web.cern.ch/operaweb/index.shtml>
- [40] see <http://www-boone.fnal.gov/>
- [41] C. Athanassopoulos *et al.*, *Phys. Rev.* **C58**, 2489 (1998); C. Athanassopoulos *et al.*, *Phys. Rev. Lett.* **81**, 1774 (1998).